

Memory effects in attenuation and amplification quantum processes

Cosmo Lupo¹, Vittorio Giovannetti², and Stefano Mancini^{1,3}

¹*School of Science and Technology, University of Camerino,
via Madonna delle Carceri 9, I-62032 Camerino, Italy*

²*NEST, Scuola Normale Superiore and Istituto Nanoscienze-CNR,
piazza dei Cavalieri 7, I-56126 Pisa, Italy*

³*INFN-Sezione di Perugia, I-06123 Perugia, Italy*

With increasing communication rates via quantum channels, memory effects become unavoidable whenever the use rate of the channel is comparable with the typical relaxation time of the channel environment. We then introduce a model of bosonic memory channel, describing correlated noise effects in quantum optical processes via attenuating or amplifying media. To study such a channel model we make use of a proper set of collective field variables, which allows us to unravel the memory effects, mapping the n -fold concatenation of the memory channel to a, unitarily equivalent, direct product of n single-mode bosonic channels. We hence estimate the channel capacities by relying on known results for the memoryless setting. Our findings show that the model is characterized by two different regimes, in which the cross-correlations induced by the noise among different channel uses are either exponentially enhanced or exponentially reduced.

PACS numbers: 03.67.Hk, 05.40.Ca, 42.50.-p, 89.70.-a

I. INTRODUCTION

Any quantum process can be described as a completely positive and trace preserving map (quantum channel) acting on the set of trace class operators (quantum states). In quantum information theory, one of the most important problems is finding the maximal rates (i.e., the capacities) at which quantum or classical information can be transmitted via quantum channels with vanishing error in the limit of large number of signals (channel uses) [1]. Earlier works on the subject focused on models where the noise affecting the communication is assumed to act independently and identically for each channel use (memoryless quantum channels). Recently, however, an increasing attention has been devoted to correlated noise models (quantum memory channels), see, e.g., [2] and references therein. Memory effects in the communication may arise when the dynamics of the media is characterized by temporal correlations which extend on timescales which are comparable with the time delay between consecutive channel uses. For instance, under certain conditions optical fibers may show relaxation times or birefringence fluctuations times longer than the separation between successive light pulses [3]. Similar effects occur in solid state implementations of quantum hardware, where memory effects due to low-frequency impurity noise produce substantial dephasing [4]. Furthermore, moving from the model introduced in [5], memory noise effects have also been studied in the context of many-body quantum systems by relating their properties to the correlations of the channel environmental state [6] or by studying the information flow in spin networks [7].

It is generally believed that memory effects should improve the information transfer of a communication line [8]. However, finding optimal encodings is rather complex and up to date only a limited number of models have been solved [2, 9, 10]. In the context of bosonic channels [11], we have recently introduced an exactly solvable model which effectively describes the transmission of signals along attenuating media characterized by finite relaxation times. It is char-

acterized by two parameters $\mu, \kappa \in [0, 1]$, enabling to describe different scenarios ranging from memoryless to inter-symbol interference channels [12], up to perfect memory configurations [13], providing thus the first comprehensive quantum information characterization of memory effects in the continuous variable setup.

In this article we show the details of such a model and we extend it to encompass amplification processes besides attenuation ones (this is formally obtained by extending the parameter space to include also $\kappa > 1$ values). For such processes we estimate the classical and the quantum capacity [14] showing their enhancement with respect to the memoryless case and proving that, for the attenuating memory channel, coherent state encoding is optimal for transmitting classical information. This is accomplished by applying suitably chosen encoding and decoding unitary transformations which allow us to *unravel* the correlations among different channel uses. In such a way the channel is mapped into a unitary equivalent one, in which noises affecting different channel uses are independent, although not identical [15]. Using this mapping, the channel capacities can be estimated by relying on known results on memoryless channels, which in the limit of large number of channel uses provide converging lower and upper bounds. Our results also allows us to point out the existence of two different regimes characterized by a threshold value of the product $\mu\kappa$. Indeed, even in the presence of amplification, for $\mu\kappa < 1$ the correlations among different channels uses induced by the channel dynamics are depressed exponentially with the distance among the uses. This strongly resemble the behavior of the so called *forgetful* memory channels, which were introduced in Ref. [2] in the context of finite dimensional systems. Vice-versa for $\mu\kappa > 1$ the memory effects, as well as the correlations between different channel uses, are exponentially enhanced by the amplification. Interestingly enough, irrespectively of these rather different behaviors the capacities of the model show no discontinuities at the critical threshold.

Even if the model we analyze is presented in an abstract setting, we believe that the results presented in the paper, as

typical in optical communication analysis [16], may have a potential impact on a variety of different realistic setups which are currently in use, ranging from fiber optics [17], to waveguide [18], up to free-space signaling [19]. Moreover, the model can be applied for describing memory effects at the interface between matter and light, e.g., in quantum repeaters and quantum memories based on ensemble of atoms, in which the state of the atomic ensemble is described in terms of an effective bosonic degree of freedom [20].

The article is organized as follows. In Sec. II we present the memory channel model. In Sec. III we introduce the technique of memory unraveling. In Sec. IV we discuss the asymptotic properties of the channel in the limit of many channel uses and characterize the threshold. The memory unraveling technique and the asymptotic properties of the channel are hence used for evaluating the classical and quantum capacity in Sec. V. In Sec. VI we argue on the forgetfulness of the model. Finally, Sec. VII we present concluding remarks.

II. THE MODEL

The most relevant effects for optical communications are the attenuation and amplification processes, which are modeled as an exchange interaction of each ingoing mode (signal) with a corresponding external bosonic mode (idler), modeling a local environment. We define a model of Gaussian memory channel by concatenating these basic transformations. An attenuation process involving a pair of ingoing modes, described through the ladder operators $\{a, a^\dagger\}$ and $\{c, c^\dagger\}$, and the corresponding outgoing modes $\{b, b^\dagger\}$, $\{d, d^\dagger\}$, is described by a unitary transformation of the form $U_{\text{BS}} = \exp(\theta a^\dagger c - \text{h.c.})$, modeling a beam-splitter mixing the two modes. In the following we assume the parameter θ to be real and positive, yielding the Heisenberg-picture transformations

$$b = U_{\text{BS}}^\dagger a U_{\text{BS}} = \cos \theta a - \sin \theta c, \quad (1a)$$

$$d = U_{\text{BS}}^\dagger c U_{\text{BS}} = \cos \theta c + \sin \theta a, \quad (1b)$$

together with their hermitian conjugates. Different choices for the parameter θ do not affect the main results of our analysis. The quantity $\cos^2 \theta$ is usually referred to as the beam-splitter transmissivity. Analogously, we will consider the linear parametric amplifier, described by a unitary operator of the form $U_{\text{LA}} = \exp(\chi a^\dagger c^\dagger - \text{h.c.})$. For simplicity we assume the parameter χ to be real and positive, even though other choices do not substantially alter our analysis. In the Heisenberg picture such a transformation acts on the ladder operators as follows

$$b = U_{\text{LA}}^\dagger a U_{\text{LA}} = \cosh \chi a + \sinh \chi c^\dagger, \quad (2a)$$

$$d = U_{\text{LA}}^\dagger c U_{\text{LA}} = \cosh \chi c + \sinh \chi a^\dagger, \quad (2b)$$

together with the hermitian conjugates. The quantity $\cosh^2 \chi$ denotes the gain of the linear amplifier. The circuitual representations of these basic unitary transformations are in Fig. 1.

To define the action of the quantum memory channel, we consider a sequence of n consecutive channel uses. Such a sequence is associated with a collection of n bosonic modes

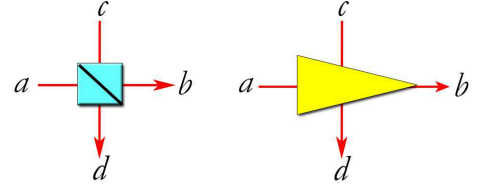


FIG. 1: (Color online.) Basic building blocks of the Gaussian memory channel, mixing the signal (represented by the horizontal lines) and the idler mode (vertical lines). On the left: the circuitual representation of the beam-splitter transformations in Eq.s (1). On the right: the circuitual representation of the linear amplifier in Eq.s (2).

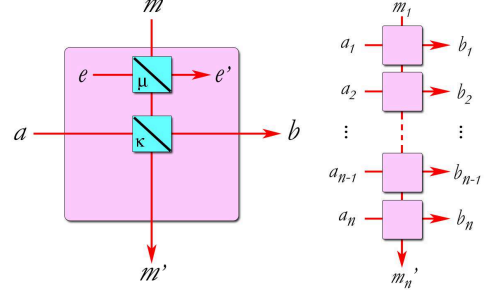


FIG. 2: (Color online.) Left: a single use of the attenuating memory channel is described as an elementary transformation which is the concatenation of two beam-splitters, respectively characterized by the transmissivities μ and κ . The first beam-splitter couples the memory mode with the local environment, the second one mixes the memory mode with the input signal. Right: n uses of the memory channel are described as the n -fold concatenation of the elementary transformation [2, 13]. The concatenation is obtained by identifying, for any j , the outgoing memory mode at the j -th channel use with ingoing memory mode at the $(j + 1)$ -th channel use. The memoryless limit is obtained when there is no information flow via the memory mode, i.e., for $\mu = 0$.

with ladder operators $\{a_j, a_j^\dagger\}_{j=1, \dots, n}$, representing the channel inputs, and the corresponding channel outputs associated with the ladder operators $\{b_j, b_j^\dagger\}_{j=1, \dots, n}$. We model the channel environment as a collection of environmental modes with $\{e_j, e_j^\dagger\}_{j=1, \dots, n}$. If the use rate of the channel becomes high enough to induce unwanted overlaps between successive uses, or to interfere with the finite relaxation time of the channel environment, then on a given use the local environment could result still “contaminated” by the previous uses. To account for such effects, in the same spirit of the Ref.s [2, 13], we introduce a *memory* mode that connects all the local environmental modes via an exchange interaction mechanism.

A single use of the memory channel is modeled by a network of linear elements: beam-splitters and/or linear amplifiers being the basic building blocks. Such an elementary transformation is depicted in Fig. 2 for the lossy memory channel, and in Fig. 3 for the amplifier one [21]. In the Schrodinger picture it is formally described by a map

$$\Phi(\rho_{a,m}) = \text{Tr}_e [U(\rho_{a,m} \otimes \rho_e)U^\dagger], \quad (3)$$

where $\rho_{a,m}$ is the ingoing state of the input and memory

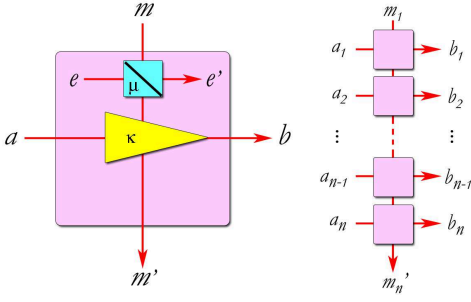


FIG. 3: (Color online.) Left: a single use of the amplifying memory channel is described as an elementary transformation which is the concatenation of a linear amplifier with gain $\kappa > 1$ and a beam-splitter with transmissivity μ . Right: the n -fold concatenation of the amplifying memory channel is obtained by identifying, for any j , the outgoing memory mode at the j -th channel use with ingoing memory mode at the $(j + 1)$ -th channel use [2, 13].

mode, and ρ_e denotes the initial state of the local environment. The unitary U is the composition of two beam-splitter unitaries for the attenuating channel (Fig. 2), or the composition of one beam-splitter and one linear amplifier for the amplifying memory channel (Fig. 3). Finally, the partial trace over the local environment accounts for the fact that its final state is ignored. In the Heisenberg picture, this elementary transformation transforms the ladder operators according to $b = U^\dagger a U$, $m' = U^\dagger m U$. For the case of the attenuating memory channel, the elementary transformation is the composition of two beam-splitters with transmissivities μ, κ (transmissivities are within the interval $[0, 1]$), hence we have

$$m' = \sqrt{\mu\kappa} m + \sqrt{1-\kappa} a + \sqrt{(1-\mu)\kappa} e, \quad (4a)$$

$$b = \sqrt{\kappa} a - \sqrt{(1-\mu)(1-\kappa)} e - \sqrt{\mu(1-\kappa)} m, \quad (4b)$$

together with the hermitian conjugate relations. Analogously, the elementary transformation in the attenuating memory channel is the composition of a beam-splitters with transmissivities μ , and a linear amplifier with gain κ , with $\kappa \in (1, \infty)$. The ladder operators hence transform according to

$$m' = \sqrt{\mu\kappa} m + \sqrt{\kappa-1} a^\dagger + \sqrt{(1-\mu)\kappa} e, \quad (5a)$$

$$b = \sqrt{\kappa} a + \sqrt{(1-\mu)(\kappa-1)} e^\dagger + \sqrt{\mu(\kappa-1)} m^\dagger, \quad (5b)$$

together with the hermitian conjugates.

The action of the memory channel upon n uses is obtained by identifying the outgoing memory mode at each channel use with the ingoing memory mode at the following one (see Figs 2, 3). Formally, this is accomplished by assigning a map of the form

$$\Phi_n[\rho_{a,m}^{(n)}] = \text{Tr}_e \left\{ \mathcal{U}_n \left[\rho_{a,m}^{(n)} \otimes \rho_e^{(n)} \right] \mathcal{U}_n^\dagger \right\}, \quad (6)$$

where $\rho_{a,m}^{(n)}$ denotes the ingoing state of the n channel input modes and of the memory mode at first channel use, and $\rho_e^{(n)}$ is the state of the n local environments. The unitary operator appearing in (6) is $\mathcal{U}_n = U_n U_{n-1} \cdots U_1$, with U_j being the unitary describing the elementary transformation in Eq. (3) applied at the j -th channel use. In the Heisenberg picture the outgoing operators m'_n, b_j 's (for $j = 1, \dots, n$), together with their hermitian conjugates, verify the identities $m'_n = \mathcal{U}_n^\dagger m_1 \mathcal{U}_n, b_j = \mathcal{U}_j^\dagger a_j \mathcal{U}_j$. For the attenuating memory channel ($\kappa \leq 1$), by iterating Eq.s (4), we have

$$m'_n = \sqrt{\mu\kappa}^n m_1 + \sqrt{1-\kappa} \sum_{j=1}^n \sqrt{\mu\kappa}^{n-j} a_j + \sqrt{(1-\mu)\kappa} \sum_{j=1}^n \sqrt{\mu\kappa}^{n-j} e_j, \quad (7)$$

$$b_j = \sqrt{\kappa} a_j + \sqrt{\mu}(\kappa-1) \sum_{h=1}^{j-1} \sqrt{\mu\kappa}^{j-h-1} a_h - \sqrt{(1-\mu)(1-\kappa)} \sum_{h=1}^j \sqrt{\mu\kappa}^{j-h} e_h - \sqrt{\mu(1-\kappa)} \sqrt{\mu\kappa}^{j-1} m_1. \quad (8)$$

Similarly, for the linear amplifier memory channel ($\kappa > 1$), from Eq.s (5) we get

$$m'_n = \sqrt{\mu\kappa}^n m_1 + \sqrt{\kappa-1} \sum_{j=1}^n \sqrt{\mu\kappa}^{n-j} a_j^\dagger + \sqrt{(1-\mu)\kappa} \sum_{j=1}^n \sqrt{\mu\kappa}^{n-j} e_j, \quad (9)$$

$$b_j = \sqrt{\kappa} a_j + \sqrt{\mu}(\kappa-1) \sum_{h=1}^{j-1} \sqrt{\mu\kappa}^{j-h-1} a_h + \sqrt{(1-\mu)(\kappa-1)} \sum_{h=1}^j \sqrt{\mu\kappa}^{j-h} e_h^\dagger + \sqrt{\mu(\kappa-1)} \sqrt{\mu\kappa}^{j-1} m_1^\dagger. \quad (10)$$

The Heisenberg-picture relations (7)-(10) will be the starting point of the information-theoretical characterization of the

memory channel which will be the aim of the following sections.

Differently from other models where the causal structure is not manifest [5, 6], this construction leads to a *non-anticipatory* channel [8] where a given input can only influence subsequent channel outputs (i.e. for each j , b_j depends only upon the a_h 's with $h \leq j$). The transmissivity μ clearly plays the role of a *memory parameter*. It can be related to the ratio between the time delay Δt between to successive channel uses and the typical relaxation time τ of the channel environment [10]: for instance we may identify $\mu \simeq \exp(-\Delta t/\tau)$. In particular, the model reduces to a memoryless (attenuating or amplifying) channel [22] for $\mu = 0$ (the input a_j only influences the output b_j), and to a channel with perfect memory [13] for $\mu = 1$ (all a_j 's interacts *only* with the memory mode). These two limiting settings respectively correspond to the regime $\Delta t \gg \tau$, and $\Delta t \ll \tau$. Intermediate configurations are associated with values $\mu \in (0, 1)$ and correspond to *inter-symbol interference* channels, for which the previous input states affect the action of the channel on the current input [12]. Of particular interest is also the case $\kappa = 0$ where Φ_n describes a *quantum shift* channel [12], where each input state is replaced by the previous one.

Finally, to exhaustively define the channel model, we have to fix the initial state of the local environmental modes $\{e_j, e_j^\dagger\}$. Different choices for the environment states lead to channels with different features. For instance, an environment in a correlated state leads to an additional source of correlated noise, similarly to the effect described by the models considered in [5, 23, 24]. In the following we assume the local environments to be in the vacuum state. With this choice, the noise caused by the interaction with the local environmental modes is limited to the shot-noise. Moreover, as we will show, this choice for the environmental states allows us to *unravel* the correlation in the memory channel [15], and to compute exactly the quantum and classical capacity by using known results for the memoryless setting [25, 26].

III. UNRAVELING THE MEMORY

The goal of this article is to estimate the classical and quantum capacity of the model of bosonic Gaussian memory channel presented above. As a first step in this direction, we consider a block of n successive channel uses and show that the application of suitably defined encoding and decoding unitary transformations allows us to *unravel* the memory effects, by mapping n uses of the memory channel into the direct product of n uncorrelated channels acting on a suitable set of collective variables [15]. Such a map defines a decomposition into ‘normal modes’ of the bosonic memory channel which, under certain conditions, is a common feature of bosonic systems described by quadratic Hamiltonians (see, e.g., [27]).

Moreover, we ought to distinguish among four different notions of (classical and quantum) capacities of the memory channel, depending whom the memory mode is assigned to [2]. Specifically, the initial and final state of the memory mode can be under the control of the sender, of the receiver, or can be ignored by both and assigned to the environment.

Here we only consider the latter case, and procrastinate the discussion of this issue to Sec. VI.

As a first step, we notice that Eq.s (8), (10) can be written in the following compact form

$$b_j = \sum_h A_{jh} a_h - \sum_h E_{jh} e_h, \quad (\kappa \leq 1), \quad (11a)$$

$$b_j = \sum_h A_{jh} a_h + \sum_h E_{jh} e_h^\dagger, \quad (\kappa > 1), \quad (11b)$$

where we have defined $e_0 := m_1$, and we have introduced the matrices A, E , whose elements are readily obtained from (8), (10). In particular, the causal structure of the memory channel implies $A_{jh} = E_{jh} = 0$ for $j < h$. By increasing values of n , two sequences of matrices of increasing dimension are defined. For each n , we consider the *singular value decomposition* of the matrix A , that is,

$$A_{jh} = \sum_{j'=1}^n O_{jj'} \sqrt{\eta_{j'}^{(n)}} O'_{j'h}, \quad (12)$$

where O, O' are unitary matrices of size n . Actually they can be assumed to be real orthogonal, for, in our construction, the matrix A has real entries. It follows from Eq.s (11) that the singular value decomposition of the matrix E reads

$$E_{jh} = \sum_{j'=1}^n O_{jj'} \sqrt{|\eta_{j'}^{(n)} - 1|} O''_{j'h}, \quad (13)$$

and that $\eta_j^{(n)} \leq 1$ for $\kappa \leq 1$, and $\eta_j^{(n)} \geq 1$ for $\kappa \geq 1$.

We hence define the following set of collective output variables

$$b_j := \sum_{j'=1}^n O_{jj'} b_{j'}, \quad (14)$$

and the input and environmental collective variables

$$a_j := \sum_{j'} O'_{jj'} a_{j'}, \quad (15a)$$

$$e_j := \sum_{j'} O''_{jj'} e_{j'}. \quad (15b)$$

These variables are named ‘collective’ since they are delocalized over different channel uses. By construction they satisfy the canonical commutation relations $[b_j, b_{j'}^\dagger] = [a_j, a_{j'}^\dagger] = [e_j, e_{j'}^\dagger] = \delta_{jj'}$. Moreover, it follows from Eq.s (11) that they verify the identities

$$b_j = \sqrt{\eta_j^{(n)}} a_j - \sqrt{1 - \eta_j^{(n)}} e_j, \quad (\kappa \leq 1), \quad (16a)$$

$$b_j = \sqrt{\eta_j^{(n)}} a_j + \sqrt{\eta_j^{(n)} - 1} e_j^\dagger, \quad (\kappa > 1). \quad (16b)$$

We denote W_A, V_B, T_E the canonical unitaries [28] that implement the transformations $a_j \rightarrow a_j = W_A^\dagger a_j W_A, b_j \rightarrow b_j = V_B^\dagger b_j V_B$ and $e_j \rightarrow e_j = T_E^\dagger e_j T_E$. We have hence shown that the channel Φ_n is unitarily equivalent to the map

$$\Phi_n[\rho_{a,m}^{(n)}] = \text{Tr}_e \left\{ \mathcal{U}'_n \left[\rho_{a,m}^{(n)} \otimes \rho_e^{(n)'} \right] \mathcal{U}'_n{}^\dagger \right\}, \quad (17)$$

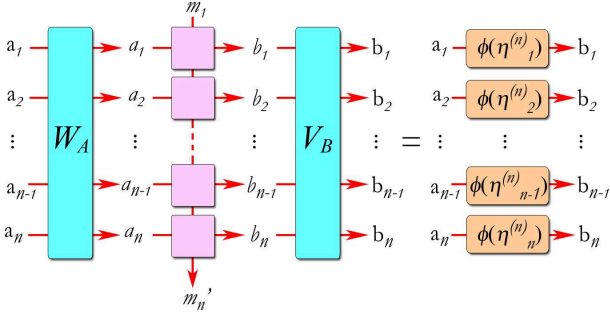


FIG. 4: (Color online.) The figure shows a circuitual representation of Eq. (18). Provided that the environmental modes and the initial memory mode are in the vacuum state, n uses of the memory channel are unitary equivalent to the direct product of n channels independently acting on the collective modes.

with $\rho_e^{(n)'} := T_E^\dagger \rho_e^{(n)} T_E$, and where the unitary transformation $U_n' := V_B U_n (W_A \otimes T_E)$ induces the linear transformations in Eq.s (16). Formally, the unitary equivalence reads

$$\Phi_n'[\rho_{a,m}^{(n)}] = V_B \Phi_n[W_A^\dagger \rho_{a,m}^{(n)} W_A] V_B^\dagger, \quad (18)$$

that is, we can treat the output states of Φ_n as output of Φ_n' by first counter-rotating the input $\rho_{a,m}^{(n)}$ by W_A (coding transformation) and then by rotating the output by V_B (decoding) [5]. Assuming then $\rho_e^{(n)}$ to be the vacuum state, we have $\rho_e^{(n)'} = \rho_e^{(n)}$ and the map (17) can be written as the direct product of independent bosonic channels, i.e.,

$$\Phi_n' = \bigotimes_{j=1}^n \phi[\eta_j^{(n)}], \quad (19)$$

with $\phi[\eta_j^{(n)}]$ being the single-mode transformations whose Heisenberg-picture description is given in Eq.s (16). A schematic representation of the encoding and decoding procedure which unravels the memory channel is shown in Fig. 4.

In conclusion, we have shown that the n -fold concatenation of the memory channel is unitarily equivalent to: n single-mode amplifier channels, each with gain $\eta_j^{(n)} \geq 1$ for $\kappa \geq 1$; n single-mode attenuating channels, each with transmissivity $\eta_j^{(n)} \leq 1$ for $\kappa \leq 1$;

IV. ASYMPTOTICAL PROPERTIES

The aim of this section is to describe the sequence of parameters $\{\eta_j^{(n)}\}_{j=1, \dots, n}$ in the limit of $n \rightarrow \infty$. The regularity of the sequence may allow us to determine converging upper and lower bounds on the channel capacities, whose evaluation will be the subject of the following section.

For all n , the parameters $\eta_j^{(n)}$ are the n eigenvalues of the real, positive matrix

$$M^{(n)} := A A^\dagger. \quad (20)$$

From Eq.s (8), (10), we obtain the following expression:

$$M_{jj'}^{(n)} = \delta_{jj'} + (\kappa_{jj'} - 1) \sqrt{\mu\kappa}^{|j-j'|}, \quad (21)$$

where

$$\kappa_{jj'} := \kappa + \mu(\kappa - 1)^2 \sum_{h=0}^{\min\{j,j'\}-2} (\mu\kappa)^h. \quad (22)$$

The asymptotic behavior of the sequence of matrices $M^{(n)}$ strongly depends upon the value of the product $\mu\kappa$. Such parameter quantifies the relation between the memory mode at two successive channel uses (see Eq.s (4a), (5a)), and allows us to split the parameter region in distinct sectors: on one hand, for $\mu\kappa < 1$ the information carried by the memory mode is attenuated and $M^{(n)}$ results in a convergent sequence of bounded operators; on the other hand, for $\mu\kappa \geq 1$ the influence of the memory mode is amplified and the sequence does not converge. In the following we will refer to these regions as *below threshold* ($\mu\kappa < 1$), *above threshold* ($\mu\kappa > 1$), and *at threshold* ($\mu\kappa = 1$).

A. Below Threshold

For $\mu\kappa < 1$ the sequence of matrices $M^{(n)}$ is *asymptotically equivalent* [29] to the (infinite) Toeplitz matrix $M^{(\infty)}$, whose elements are

$$M_{jj'}^{(\infty)} := M_{j-j'}^{(\infty)} = \delta_{jj'} + [\kappa^{(\infty)} - 1] \sqrt{\mu\kappa}^{|j-j'|}, \quad (23)$$

with

$$\kappa^{(\infty)} := \lim_{\min\{j,j'\} \rightarrow \infty} \kappa_{jj'} = \kappa + \frac{\mu(\kappa - 1)^2}{1 - \mu\kappa}. \quad (24)$$

Following Ref. [29] the asymptotic distribution of the eigenvalues of the matrix $M^{(n)}$ can then be expressed in terms of the continuous function obtained by Fourier transforming the elements of the matrix $M^{(\infty)}$, i.e.,

$$\eta(z) = \sum_{j=-\infty}^{\infty} M_j^{(\infty)} e^{izj/2} = \left| \frac{\sqrt{\mu} - \sqrt{\kappa} e^{iz/2}}{1 - \sqrt{\mu\kappa} e^{iz/2}} \right|^2, \quad (25)$$

with $z \in [0, 2\pi]$ [30]. The connection between the parameters $\eta_j^{(n)}$ and the function (25) is formalized by the Szegő theorem [29] which states that, for any smooth function F , we have

$$\lim_{n \rightarrow \infty} \frac{1}{n} \sum_{j=1}^n F[\eta_j^{(n)}] = \int_0^{2\pi} \frac{dz}{2\pi} F[\eta(z)]. \quad (26)$$

B. Above Threshold

When the channel operates above threshold the sequence of matrices does not converge. For $\mu\kappa > 1$ we find it convenient to rewrite Eq. (21) as the sum of two terms:

$$M^{(n)} = c^{(n)} P^{(n)} + \Delta M^{(n)}, \quad (27)$$

where $P^{(n)}$ is a sequence of rank one projectors, $c^{(n)}$ is a diverging sequence of positive real numbers, and $\Delta M^{(n)}$ is a sequence of matrices which asymptotically converges towards the (infinite) Toeplitz matrix $\Delta M^{(\infty)}$, with entries

$$\Delta M_{jj'}^{(\infty)} = \frac{(1-\mu)(\kappa-1)}{\mu\kappa-1} \frac{1}{\sqrt{\mu\kappa}^{|j-j'|}}. \quad (28)$$

The explicit expressions of the projectors $P^{(n)}$ and of the matrices $\Delta M^{(n)}$ are reported in Appendix A. One can easily verify that in the asymptotic limit of $n \rightarrow \infty$ they commute (or, to say it more formally, that their commutator is asymptotically equivalent to the null matrix). We conclude that the spectrum of the matrices (21) is asymptotically composed of one diverging eigenvalue [from the diverging sequence $c^{(n)}$] and of the asymptotic distribution of the eigenvalues of the infinite Toeplitz matrix (28). Similarly to the below threshold case, the latter can be calculated by Fourier transforming: we hence find that it is described by the function in Eq. (25), extended to the region $\mu\kappa > 1$.

C. At threshold

At the threshold value, $\mu\kappa = 1$, the matrix $M^{(n)}$ can be expressed as

$$M_{jj'}^{(n)} = \delta_{jj'} + (1-\mu) + \frac{(1-\mu)^2}{\mu} \min\{j, j'\}. \quad (29)$$

A part from the trivial case $\mu = 1$ where $M^{(n)}$ coincides with the identity operator (perfect channel), the analysis of the asymptotic behavior is rather cumbersome (for instance, it is not possible to identify a single diverging eigenvalue). We thus resort on numerical diagonalization of the sequence of matrices. This shows that the finite part of the spectrum is again well fitted by the distribution Eq. (25), extended to the manifold with $\mu\kappa = 1$.

V. CAPACITIES

Equation (19) suggests the possibility of computing the classical and quantum capacity of the memory channel by applying the results for the memoryless multi-mode channels [25, 26]. To do so however, we have first to deal with the fact that the single-mode channels forming Φ'_n are not necessarily identical. Therefore the map (19) is not memoryless in a strict sense. To cope with this problem we will construct two collections of memoryless channels which upper and lower bound the capacity of the memory channel, and then we will use the asymptotic distribution (25) to show that, for large n , they converge toward the same quantity.

We proceed as follows. For n uses of the memory channel we arrange the single-mode channels $\{\phi(\eta_j^{(n)})\}$ in such a way that the corresponding parameters $\eta_j^{(n)}$ are ordered monotonically. We further divide the single-mode channels in P blocks,

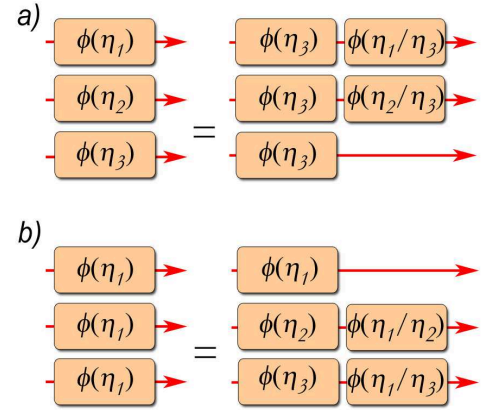


FIG. 5: (Color online.) The figure shows a circuitual representation of the law of composition of attenuating or amplifying bosonic channels. To fix the ideas, let us consider a sequence of $n = 3$ uses of the memory channel, associated to three parameters η_j . For the attenuating channel, let us assume $\eta_1 \leq \eta_2 \leq \eta_3 \leq 1$. It follows that: (a) the rate of information transmission cannot be greater than the one of the channel with all the transmissivities equal to η_3 ; and (b) it cannot be smaller than the one with all the transmissivities equal to η_1 . The same bounds hold true for the amplifying channel, assuming $\eta_1 \geq \eta_2 \geq \eta_3 \geq 1$.

each containing $\ell = n/P$ channels, and define the infimum and supremum for each block, i.e.

$$\underline{\eta}_p^{(P)} = \inf_n \inf_{(p-1)\ell < j \leq p\ell} \eta_j^{(n)}, \quad (30)$$

$$\overline{\eta}_p^{(P)} = \sup_n \sup_{(p-1)\ell < j \leq p\ell} \eta_j^{(n)}. \quad (31)$$

It is worth noticing that, for any integer P and independently on n , the two collections of parameters, $\{\overline{\eta}_p^{(P)}\}_{p=1, \dots, P}$ and $\{\underline{\eta}_p^{(P)}\}_{p=1, \dots, P}$, identify two memoryless multi-mode bosonic channels [25]. Such channels are either attenuating channels, for $\kappa \leq 1$, or amplifying channels for $\kappa > 1$. We also remark that $\phi(\eta)\phi(\eta') = \phi(\eta\eta')$, that is, the composition of two attenuating (amplifying) channels with transmissivities (gains) η, η' , is an attenuating (amplifying) channel with transmissivity (gain) $\eta'' = \eta\eta'$. Since the capacities do not increase under composition of channels, we conclude that, for any P , the capacity of the memory channel is bounded by the capacities of the memoryless multi-mode channels identified by the set of parameters $\{\overline{\eta}_p^{(P)}\}_{p=1, \dots, P}$ and $\{\underline{\eta}_p^{(P)}\}_{p=1, \dots, P}$. (See Fig. 5 for an illustrative example.)

As customary, to avoid unphysical results when discussing the classical capacity of bosonic channels, we will adopt suitable constraints on the input encodings (this can be avoided when dealing with the quantum capacity, since typically it does not diverge even for unbounded inputs [22, 26]). Here we compute the constrained classical capacity under the condition

$$\frac{1}{n} \sum_{j=1}^n \text{Tr} [\rho^{(n)} a_j^\dagger a_j] \leq N, \quad (32)$$

where $\rho^{(n)}$ is the ensemble of input states over n channel uses, the parameter N expresses the maximum number of mean excitations per mode in average, and the constraint is intended to hold for all values of n . It is important to notice that the encoding transformation used for unraveling the memory channel [Eq. (15a)] preserves the input energy (this simply follows from the fact that the matrix O' is orthogonal). Thus, the form of the energy constraint is preserved when written in terms of the collective input variables $\{a_j, a_j^\dagger\}$, i.e.,

$$\frac{1}{n} \sum_{j=1}^n \text{Tr} \left[\rho^{(n)} a_j^\dagger a_j \right] \leq N. \quad (33)$$

A. Quantum capacity

The quantum capacity of the memoryless attenuating and amplifying channels has been derived in [26]. By relying on additivity arguments [31], this result is readily extensible to the case of memoryless multimode channels [25].

For the sake of simplicity, we focus on the limit of unbounded input energy (i.e., $N \rightarrow \infty$), which leads to the function [26]

$$q(\eta) := \max\{0, \log_2 \eta - \log_2 |\eta - 1|\}. \quad (34)$$

We hence obtain, for any P , the expressions $\frac{1}{P} \sum_p q[\underline{\eta}_p^{(P)}]$ and $\frac{1}{P} \sum_p q[\overline{\eta}_p^{(P)}]$ for the quantum capacity (per input mode) of the multi-mode channels, respectively characterized by the parameters $\underline{\eta}_p^{(P)}$ and $\overline{\eta}_p^{(P)}$. Then, we can construct the following upper and lower bounds for the quantum capacity of the memory channel:

$$\underline{Q}^{(P)} = \begin{cases} \frac{1}{P} \sum_p q[\underline{\eta}_p^{(P)}], & (\kappa \leq 1), \\ \frac{1}{P} \sum_p q[\overline{\eta}_p^{(P)}], & (\kappa > 1), \end{cases} \quad (35a)$$

$$\overline{Q}^{(P)} = \begin{cases} \frac{1}{P} \sum_p q[\overline{\eta}_p^{(P)}], & (\kappa \leq 1), \\ \frac{1}{P} \sum_p q[\underline{\eta}_p^{(P)}], & (\kappa > 1), \end{cases} \quad (35b)$$

so that

$$\underline{Q}^{(P)} \leq Q \leq \overline{Q}^{(P)}. \quad (36)$$

By varying the value of the integer P , we hence obtain a family of lower and upper bounds on the quantum capacity Q of the memory channel.

In the limit $P \rightarrow \infty$, the collections of parameters $\{\underline{\eta}_p^{(P)}\}$, $\{\overline{\eta}_p^{(P)}\}$ may approach a limiting distribution. Clearly, this is the case when the channel operates below threshold, with the limiting distribution given in Eq. (25). It follows that the upper and lower bounds converge towards a same quantity in the limit $P \rightarrow \infty$, and by applying the Szegő theorem [Eq. (26)] we can write

$$Q = \int_0^{2\pi} \frac{dz}{2\pi} q[\eta(z)]. \quad (37)$$

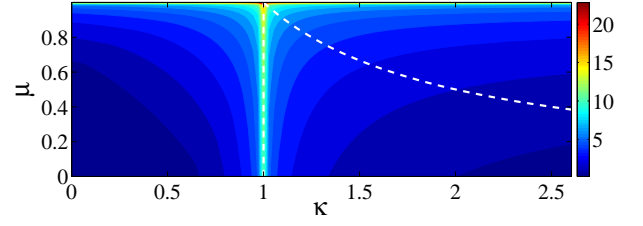


FIG. 6: (Color online.) The contour plot shows the quantum capacity (measured in qubits per channel use) of the memory channel as function of the amplifying/attenuating factor κ and of the memory parameter μ . The quantum capacity is computed using Eq. (37), which diverges logarithmically for $\mu \rightarrow 1$ and for $\kappa \rightarrow 1$. The dashed lines denote the boundaries among different regions, from left to right: attenuating channel, amplifying channel below threshold, amplifying channel above threshold.

It is worth remarking that the Szegő theorem can be applied on smooth functions. Since the function in Eq. (34) is singular for $\eta = 1$, we deduce that the expression in Eq. (37) coincides with the quantum capacity of the memory channel if the parameters $\{\underline{\eta}_p^{(P)}\}$, $\{\overline{\eta}_p^{(P)}\}$ do not approach the unit value for all the values of P and p . By numerical evaluation of the distribution of the parameters, we found evidences that this is the case for the setting in which both initial and final memory modes are assigned to the environment (see Sec. III). As discussed in the Sec. VI, the expression in (37) does not coincide with the channel capacity if the final memory mode is assigned to the receiver.

Above threshold, the distribution of eigenvalues is composed by a continuous part, described by Eq. (25), and by one diverging eigenvalue. However, for the form of the function (34), the latter does not contribute to the channel capacity. In conclusion, the quantity in Eq. (37) expresses the quantum capacity of the memory channel both below and above threshold, proving that Q keeps no record of such discontinuity. A plot of Eq. (37) as a function of the parameters μ , κ is reported in Fig. 6 (for $\kappa > 1$, the dashed line represents the threshold value $\kappa\mu = 1$).

B. Classical capacity

Similarly to the previous case, for the classical capacity we consider a family of bounds constructed by introducing a proper set of memoryless channels. For P integer, this yields the inequalities

$$\underline{C}^{(P)} \leq C \leq \overline{C}^{(P)}, \quad (38)$$

where the bounds are computed from the classical capacity of the memoryless multi-mode channels defined by the sequence of parameters $\{\underline{\eta}_p^{(P)}\}$, $\{\overline{\eta}_p^{(P)}\}$.

Let us first consider the case of the attenuating memory channel (i.e., $\kappa \leq 1$) for which exact results can be derived. The constrained classical capacity of the memoryless multi-mode channel has been derived in [25], from which we can

write

$$\underline{C}^{(P)} = \frac{1}{P} \sum_{p=1}^P g[\underline{\eta}_p^{(P)} \underline{N}_p], \quad (39a)$$

$$\overline{C}^{(P)} = \frac{1}{P} \sum_{p=1}^P g[\overline{\eta}_p^{(P)} \overline{N}_p], \quad (39b)$$

where

$$g(x) := (x+1) \log_2(x+1) - x \log_2 x. \quad (40)$$

The positive parameters $\{\underline{N}_p\}$, $\{\overline{N}_p\}$ describe the optimal distributions of the excitation numbers over the collective input modes. For any P the optimal distributions can be computed by Lagrange method [25]. In terms of a Lagrange multiplier L , the optimal distribution is

$$\underline{N}_p = \left\{ \underline{\eta}_p^{(P)} \left[2^{L/\underline{\eta}_p^{(P)}} - 1 \right] \right\}^{-1}, \quad (41)$$

and the value of the multiplier is found accordingly to the constraint (33), which reads

$$\frac{1}{P} \sum_{p=1}^P \underline{N}_p = N, \quad (42)$$

and analogously for the distribution $\{\overline{N}_p\}$.

Taking the limit $P \rightarrow \infty$ and applying (26) we notice that the two bounds (39) converge to the same quantity. Therefore we conclude that

$$C = \int_0^{2\pi} \frac{dz}{2\pi} g[\eta(z)N(z)], \quad (\kappa \leq 1). \quad (43)$$

The function $N(z)$ represents the optimal excitation number distribution; by taking the limit of Eq.s (41) and (42), it can be computed as

$$N(z) = \left\{ \eta(z) \left[2^{L/\eta(z)} - 1 \right] \right\}^{-1}, \quad (44)$$

where the value of the Lagrange multiplier is determined by the implicit equation

$$\int_0^{2\pi} \frac{dz}{2\pi} N(z) = N. \quad (45)$$

In some limiting cases Eq. (43) admits a close analytical solution. For instance in the memoryless configuration $\mu = 0$, we get $\eta(z) = \kappa$, $N(z) = N$ and thus correctly $C = g(\kappa N)$ [25]. Vice-versa for $\kappa = 1$ (noiseless channel) or $\mu = 1$ (perfect memory channel) we have $\eta(z) = 1$, $N(z) = N$ and thus $C = g(N)$ (perfect transfer). Finally for $\kappa = 0$ (quantum shift channel) we get $\eta(z) = \mu$, $N(z) = N$ and thus $C = g(\mu N)$. For generic values of the parameters the resulting expression can be numerically evaluated, showing an increase of C for increasing memory μ .

Let us now consider the amplifying channel model, obtained for $\kappa > 1$. This is intrinsically more complex than

the previous one, since in this case no exact results are known even in the memoryless case. Consequently Eq. (38) will only provide a lower bound on the real capacity C of our memory channel. For this purpose we construct a lower bound for the classical capacity $\underline{C}^{(P)}$ of the memoryless multi-mode channel by restricting the coding strategy to only Gaussian inputs [22] (it is worth noticing that such bound is typically considered to be tight). This yields

$$\underline{C}^{(P)} \geq \frac{1}{P} \sum_{p=1}^P g \left[\overline{\eta}_p^{(P)} (\overline{N}_p + 1) + 1 \right] - g \left[\overline{\eta}_p^{(P)} - 1 \right]. \quad (46)$$

The optimal distribution of the excitation numbers is computed by Lagrange method. In terms of a Lagrange multiplier L , it reads

$$\overline{N}_p = \left\{ \overline{\eta}_p^{(P)} \left[1 - 2^{-L/\overline{\eta}_p^{(P)}} \right] \right\}^{-1} - 1. \quad (47)$$

We have hence obtained a family of lower bounds on the memory channel capacity. By taking the limit $P \rightarrow \infty$ we get

$$C \geq \int_0^{2\pi} \frac{dz}{2\pi} (g \{ \eta(z) [N(z) + 1] + 1 \} - g [\eta(z) - 1]), \quad (48)$$

where $\eta(z)$ is the asymptotic function (25), and the optimal asymptotic distribution of excitation numbers is given by

$$N(z) = \left\{ \eta(z) \left[1 - 2^{-L/\eta(z)} \right] \right\}^{-1} - 1. \quad (49)$$

We stress that, as in the analysis of the quantum capacity Q , the expression given in Eq. (48) holds also above threshold. Indeed due to the form of the function (46), the diverging eigenvalues give a vanishing contribution to the lower bound on the classical capacity and can thus be neglected. Figure 7 shows the (lower bound on the) classical capacity of the memory channel as function of the channel parameters μ, κ .

VI. FORGETFULNESS OF THE MEMORY CHANNEL

According to Ref. [2], when dealing with memory channels one has to distinguish among four different settings, which may lead to different values of the channel capacities, depending whom the initial and final memory modes are assigned to. We denote the four possible settings by the label XY : $XY = AE$ (the initial memory mode is assigned to the sender and the final one to the environment), AB (the initial and final memory modes are assigned respectively to the sender and to the receiver), EB (initial memory mode to the environment and final one to the receiver), and EE (both initial and final memory modes are assigned to the environment). If the initial memory mode is assigned to the environment, the channel capacities may also depend on the memory initialization. [We remind that the calculations presented in the previous section have been performed in the configuration EE assuming the memory mode to be initialized in the vacuum].

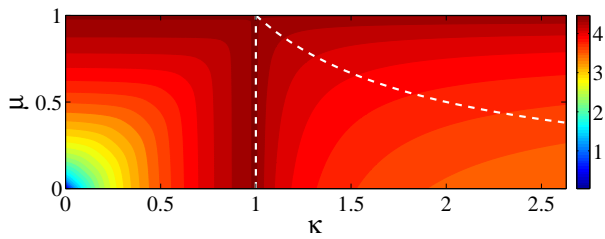


FIG. 7: (Color online.) The contour plot refers to the classical capacity (measured in bits per channel use) of the memory channel as function of the amplifying/attenuating factor κ and of the memory parameter μ , under the constraint (32) with $N = 8$. For the attenuation channel ($\kappa \leq 1$), the classical capacity of the memory channel is plotted, using Eq. (43). For the amplifying channel ($\kappa > 1$), the plotted quantity is a lower bound on the classical capacity. The dashed lines denote the boundaries among different regions, from left to right: attenuating channel, amplifying channel below threshold, amplifying channel above threshold.

The notion of *forgetfulness*, and hence the class of forgetful memory channels, has been introduced in [2] for quantum channels acting on finite-dimensional Hilbert spaces. Forgetful channels are characterized by several remarkable properties, in particular the capacities of those channels do not depend on the setting XY and on the initialization of the memory mode. Let us notice that our model is defined on an infinite-dimensional Hilbert space, and hence the notion of forgetfulness cannot be directly applied. However, we can argue on the forgetfulness of the channel if an effective cutoff on the bosonic Hilbert space is introduced. To prove the forgetfulness it is sufficient to show that, in the limit of $n \rightarrow \infty$, the final state of the memory mode is independent, in the sense specified in Ref. [2], on the memory initialization. Indeed, the presence of the exponential factor $\sqrt{\mu\kappa^n}$ in (7), (9) suggests that the channel is forgetful when $\mu\kappa < 1$, that is, when operating below threshold. We can prove that this holds true restricting to Gaussian states with bounded energy. To fix the ideas, let us consider the case of the attenuating channel. The transformation (7) reads

$$m'_n = \sqrt{\mu\kappa^n} m_1 + \mathbf{X}^T \mathbf{a} + \mathbf{Y}^T \mathbf{e}, \quad (50)$$

where $\mathbf{a} := (a_1, \dots, a_n)^T$, $\mathbf{e} := (e_1, \dots, e_n)^T$, and the form of the vectors \mathbf{X} , \mathbf{Y} can be deduced from (7). A Gaussian state of the initial memory mode, the input and the environmental modes, is characterized by the first moments $\langle m_1 \rangle$, $\langle \mathbf{a} \rangle$, $\langle \mathbf{e} \rangle$, and by the covariance matrix

$$V = \begin{pmatrix} V_m & C^T & D^T \\ C & V_a & 0 \\ D & 0 & V_e \end{pmatrix}, \quad (51)$$

where the off-diagonal terms account for possible correlations of the initial memory mode with the input and environment modes. After n uses of the channel, the state of the final memory mode is Gaussian with first moment

$$\langle m'_n \rangle = \sqrt{\mu\kappa^n} \langle m_1 \rangle + \mathbf{X}^T \langle \mathbf{a} \rangle + \mathbf{Y}^T \langle \mathbf{e} \rangle, \quad (52)$$

and covariance matrix

$$V'_m = (\mu\kappa)^n V_m + \sqrt{\mu\kappa^n} (\mathbf{X}^T C + \mathbf{Y}^T D + C^T \mathbf{X} + D^T \mathbf{Y}) + \mathbf{X}^T V_a \mathbf{X} + \mathbf{Y}^T V_e \mathbf{Y}. \quad (53)$$

The presence of the exponential factors in (52), (53) guarantees the forgetfulness of the channel as long as the energy is bounded, e.g., subjected to a constraint of the form

$$\frac{\langle m_1^\dagger m_1 \rangle + \sum_{j=1}^n \langle a_j^\dagger a_j \rangle}{n+1} \leq N. \quad (54)$$

The same argument can be provided for the amplifying channel, as long as it operates below threshold. It is finally worth reminding that a first step towards the extension of the notion of forgetfulness to the domain of continuous variables has been made in [23]. However, we notice that this extension is not straightforward if the full infinite dimensional Hilbert space is considered. To illustrate this issue we consider the computation of the quantum capacity, with unbounded input energy, in the generic XY setting. By inspection of Figs. 2, 3, it is immediate to see that in the AB and EB settings, where the final memory mode is assigned to the receiver, at least one input mode is perfectly transmitted, leading to an infinite value of the quantum capacity for any value of the parameters μ, κ . On the other hand, we have shown in Sec. VA that the quantum capacity is finite in the EE setting (the same can be shown in the EB setting) for all values of the parameters, provided $\mu, \kappa \neq 1$.

VII. CONCLUSIONS

We have introduced and characterized a model for memory effects in attenuation and amplification quantum channels. Our findings show that the presence of memory always increases the quantum capacity of the communication line and may increase the classical one.

Interestingly enough, the highest rates of classical communication are reached without the use of entangled codewords. For the attenuating channel, the optimal encoding strategy for the memoryless channels which bound Φ_n makes use of coherent states [25]. Since the latter are preserved by the encoding transformation W_A our results prove, as a byproduct, the optimality of coherent state encoding for the presented memory channel.

We emphasize the use of the memory unraveling technique [15], which may allow us to evaluate the channel capacity without relying on the channel forgetfulness. This shows that the unraveling of the memory could have a much broader impact than the results we have presented here. In particular it may find applications on other contexts, e.g., reaching beyond current restricted models that involve statistically independent errors and are often inapplicable to real physical systems. For instance, the model could be easily adapted to describe situation in which temporal (causal) correlations between the channel uses are replaced by spatial ones or to deal with physical models where the underlying noise is more complicated than

attenuation (e.g., a stream of two level atoms injected through a superconducting cavity). The model can also be applied to describe memory effects in quantum repeaters and quantum memories with atomic ensembles, where, via the Holstein-Primakoff transformation [32], the interaction between matter and light can be modeled as a formal beam-splitter (or linear-amplifier) Hamiltonian [20]. An imperfect swap operation between matter and light can be described by a beam-splitter with non-unit transmissivity, which in turn may causes memory effects.

Appendix A: Explicit expressions

Writing the elements of the projector $P_{jj'}^{(n)}$ as $\psi_j \psi_{j'}$, the explicit expressions for the quantities on the right hand side of Eq. (27) are as follows

$$c^{(n)} := \frac{\kappa(\kappa-1)(1-\mu)^2}{(\mu\kappa-1)^2} \left[1 - \frac{1}{(\mu\kappa)^n} \right] + \frac{\mu(\kappa-1)}{(\mu\kappa-1)^2} [(\mu\kappa)^n - 1] - \frac{2(1-\mu)(\kappa-1)}{\mu\kappa-1} n ,$$

$$\psi_j := \frac{1}{\sqrt{c^{(n)}}} \left[\sqrt{\frac{\kappa-1}{\kappa(\mu\kappa-1)}} \sqrt{\mu\kappa^j} - (1-\mu) \sqrt{\frac{\kappa(\kappa-1)}{\mu\kappa-1}} \frac{1}{\sqrt{\mu\kappa^j}} \right] ,$$

and

$$\Delta M_{jj'}^{(n)} := \frac{(1-\mu)(\kappa-1)}{\mu\kappa-1} \frac{1}{\sqrt{\mu\kappa^{|j-j'|}}} - (1-\mu)^2 \frac{\kappa(\kappa-1)}{\mu\kappa-1} \frac{1}{\sqrt{\mu\kappa^{j+j'}}} .$$

Acknowledgments

The research leading to these results has received funding from the European Commission's seventh Framework Programme (FP7/2007-2013) under grant agreements no. 213681, and by the Italian Ministry of University and Research under the FIRB-IDEAS project RBID08B3FM.

-
- [1] M. Hayashi, *Quantum Information: An Introduction*, Springer, Berlin 2006.
- [2] D. Kretschmann and R. F. Werner, Phys. Rev. A **72**, 062323 (2005).
- [3] K. Banaszek, A. Dragan, W. Wasilewski, and C. Radzewicz, Phys. Rev. Lett. **92**, 257901 (2004); R. Demkowicz-Dobrzański, P. Kolenderski, K. Banaszek, Phys. Rev. A **76**, 022302 (2007).
- [4] E. Paladino, L. Faoro, G. Falci, and R. Fazio, Phys. Rev. Lett. **88**, 228304 (2002); Y. Hu, Y.-F. Xiao, Z.-W. Zhou, and G.-C. Guo, Phys. Rev. A **75**, 012314 (2007).
- [5] V. Giovannetti and S. Mancini, Phys. Rev. A **71**, 062304 (2005).
- [6] M. B. Plenio and S. Virmani, Phys. Rev. Lett. **99**, 120504 (2007); New J. Phys. **10**, 043032 (2008); D. Rossini, V. Giovannetti, and S. Montangero, *ibid.* **10**, 115009 (2008); F. Caruso, V. Giovannetti, and G. M. Palma, Phys. Rev. Lett. **104**, 020503 (2010).
- [7] V. Giovannetti and R. Fazio, Phys. Rev. A **71**, 032314 (2005); D. Rossini, V. Giovannetti and R. Fazio, Int. J. of Quantum Inf., **5** 439 (2007); A. Bayat, D. Burgarth, S. Mancini, and S. Bose, Phys. Rev. A , **77**, 050306(R) (2008); V. Giovannetti, D. Burgarth, and S. Mancini, *ibid.* **79**, 012311 (2009).
- [8] R. G. Gallager, *Information Theory and Reliable Communication* (Wiley, New York, 1968).
- [9] N. Datta and T. C. Dorlas, J. Phys. A: Math. Theor. **40**, 8147 (2007); A. D' Arrigo, G. Benenti, and G. Falci, New J. Phys. **9**, 310 (2007).
- [10] V. Giovannetti, J. Phys. A **38**, 10989 (2005).
- [11] C. Lupo, V. Giovannetti and S. Mancini, Phys. Rev. Lett. **104**, 030501 (2010).
- [12] G. Bowen, I. Devetak and S. Mancini, Phys. Rev. A **71**, 034310 (2005).
- [13] G. Bowen and S. Mancini, Phys. Rev. A **69**, 012306 (2004).
- [14] Similar results can be also derived for their entanglement assisted counterparts.
- [15] C. Lupo, S. Mancini, Phys. Rev. A **81**, 052314 (2010).
- [16] C. M. Caves and P. D. Drummond, Rev. Mod. Phys. **66**, 481 (1994).
- [17] N. Gisin, G. Ribordy, W. Tittel, and H. Zbinden, Rev. Mod. Phys. **74**, 145 (2002).
- [18] S. Tanzilli, *et al.*, Eur. Phys. J. D, **18**, 155 (2002).
- [19] V. W. S. Chan, J. Lightw. Technol., **24**, 4750 (2006); A. Fedrizzi, *et al.*, Nat. Phys. **5**, 389 (2009).
- [20] K. Hammerer, A. S. Sørensen, E. S. Polzik, Rev. Mod. Phys. **82**, 1041 (2010).
- [21] The methods developed in Sec.s III-V may as well be applied to models of memory channels defined by different combinations of the linear elements.
- [22] A. S. Holevo and R. F. Werner, Phys. Rev. A **63**, 032312 (2001).
- [23] C. Lupo, L. Memarzadeh and S. Mancini, Phys. Rev. A **80**, 042328 (2009).
- [24] C. Lupo, O. V. Pilyavets, S. Mancini, New J. Phys. **11**, 063023 (2009).
- [25] V. Giovannetti, S. Guha, S. Lloyd, L. Maccone, J. H. Shapiro, and H. P. Yuen, Phys. Rev. Lett. **92**, 027902 (2004); V. Giovannetti, S. Lloyd, L. Maccone, and P. W. Shor, Phys. Rev. A **68**, 062323 (2003).
- [26] M. M. Wolf, D. Pérez-García and G. Giedke, Phys. Rev. Lett. **98**, 130501 (2007).
- [27] A. I. Lvovsky, W. Wasilewski, K. Banaszek, J. Mod. Opt. **54**, 721 (2007).
- [28] A. S. Holevo, *Probabilistic and Statistical Aspects of Quantum Theory* (Amsterdam: North-Holland, 1982).
- [29] R. M. Gray, *Toeplitz and Circulant Matrices: A Review*, (Now Publishers, Norwell, Massachusetts, 2006).
- [30] The factor 1/2 in the right hand side term of Eq. (25) has been introduced to make $\eta(z)$ monotonic in z .
- [31] F. Caruso, V. Giovannetti, Phys. Rev. A **74**, 062307 (2006).
- [32] T. Holstein, H. Primakoff, Phys. Rev. **58**, 1098 (1940).